Indian Journal of Biochemistry & Biophysics
Vol. 57, April 2020, pp. 151-157

Thiol stabilized copper nanoparticles exert antimicrobial properties by preventing cell division in *Escherichia coli*

Ganesh Kumar N[1], Satya Deo Pandey[2], Sathi Mallick[2], Sudip Kumar Ghosh[2], Panchanan Pramanik[3]& Anindya S Ghosh[2]*

[1]Advanced Technology Development Centre; [2]Department of Biotechnology; [3]Department of Chemistry, Indian Institute of Technology Kharagpur, Kharagpur-721 302, West Bengal, India

Received 03 September 2019; *revised 16 October 2019*

The uses of metallic nanoparticles have gained importance as one of the therapeutic options to treat infections. Here, we synthesized stable copper nanoparticles (CuNPs) using Thiosalicylic acid and assessed their antimicrobial activities against various Gram-negative bacteria. The synthesized CuNPs had absorption maxima of 570 nM with a size range of 5-11 nM and face-centred cubic (Fcc) crystal structure. The bacterial cells in their planktonic and sessile forms were susceptible to CuNPs. The nanoparticles did not show any cytotoxicity to murine macrophages (RAW264.7) below 60 µg/mL. However, the expression of oxidative stress defence gene *ahpC* revealed the possibility of ROS generation upon treatment with CuNPs. Interestingly, the cell division proteins like, FtsZ and FtsI were destabilized in the presence of CuNPs which in turn inhibited bacterial cell division. In conclusion, it may be stated that the synthesized CuNPs can kill bacteria by arresting cell division and/or by ROS generation.

Keywords:Biopolymers, Cell division, Copper-nanoparticle, Cytotoxicity, HR-TEM, ROS

Multi-drug resistant (MDR) bacterial population pose a global threat to the conventional antimicrobial chemotherapy, which in turn affects our survival[1]. Therefore, it is essential to find alternative approaches to curb bacterial infections. During the last decade, Nano-particles have gained importance because of their unique physical, chemical and biological properties[2]. Among them metal and metal oxide nanoparticles are of choice to be used as an antimicrobial agent, *e.g.*, silver nanoparticles (AgNPs)[3,4]. It is believed that the smaller the particle size, the higher its antimicrobial activity. Though AgNPs act as antimicrobials, they are expensive and have serious side effects like argyria[5]. Hence, there is a need for doing alternative metals. Recently, the interest has shifted to metal oxides of copper, zinc[6], bismuth, and titanium because of their easy availability and exceptional features. These materials exhibit unique mechanical, optical and biological properties[7]which make them potential candidates for biomedical applications[8,9] of which metallic copper composites have been studied in antimicrobial dressings and textile coatings[10,11,12,13].

Synthesis of CuNPs has posed challenges like oxidation of copper in air and aggregation of the particles[14,15,16]. However, nitrogen gas provides an inert environment, the capping/ stabilizing agents like polymers and biopolymers (gelatine) are thought to prevent such oxidation by providing steric or ionic stability to the CuNPs[14]. The CuNPs have been reported to show excellent antimicrobial activity against Gram-negative bacteria. It is thought that CuNPs may affect cell-wall biosynthesis by preventing cell-wall remodelling enzymes or by the generation of reactive oxygen species (ROS) that can degrade genomic DNA or/and denature the sulphur-containing proteins'[17]. Here, we have synthesized CuNPs using strong stabilizing agents like Thiosalicylic acid and attempted to explore the

*Correspondence:
Phone: +91-9830696807 (Mob)
Email: anindyain@yahoo.com

Abbreviations: *AhpC*,alkyl hydroperoxide reductase; CuNPs, Copper nanoparticles; DLS, Dynamic light scattering; FCC, Face centred cubic; FTIR, Fourier transform infrared spectroscopy; HR-TEM, High-resolution Transmission Electron Microscope; IPTG, isopropyl-β-D-thiogalactoside; MBEC, Minimal biofilm eradication concentration; MDR, Multi-drug resistant; MIC, Minimal inhibitory concentration; MTT, 3-(4,5-dimethylthiazol-2-yl)-2,5-diphenyltetrazolium bromide; ROS, Reactive oxygen species; SAED, The selected area electron diffraction; TTC, Triphenyl tetrazolium chloride; XRD, X-ray diffraction

molecular basis of its bactericidal action.

Materials and Methods

Unless otherwise specified all the chemicals for CuNPs synthesis were purchased from Merck, Mumbai, India and Sigma Aldrich, California, USA. Bacterial strains used (Table 1) were either laboratory strains or purchased from MTCC, India. The plasmids for FtsZ-GFP and FtsI-GFP were a generous gift from Kevin D. Young (Professor, Department of Microbiology and Immunology,College of Medicine, the University of Arkansas for Medical Sciences, 4301W, Markham St.Little Rock, AR 72205, USA).

Synthesis and characterization of CuNPs

CuNPs synthesis and characterization

Thiosalicylic acid in 70% ethanol was added dropwise to 5% (*w/v*) copper sulphate solution ($CuSO_4.5H_2O$) until the blue colour disappeared and subsequently, hydrazine hydrate was added to the mixture until the colour changed to yellowish-orange. The reaction mixture was kept for 3 h at room temperature until it obtained a brick red colour. The solution was kept overnight for maturation and stored for further studies as Nano-fluid.

The absorption maxima of synthesized CuNPs were determined through spectral analysis, particle size was determined using dynamic light scattering (DLS, Horiba Scientific, Japan) and High-resolution Transmission Electron Microscope (HR-TEM, Jeol, Tokyo, Japan). The X-ray diffractometer (XRD, Shimadzu Corporation, Kyoto, Japan) was used to analyse the crystal faces. Fourier transform infrared spectroscopy (FTIR) (Perkin Elmer, Kyoto, Japan) analysis of the CuNPs was done by pelleting the particle with KBr with the motorized pelleting machine.

Table 1 — Values of CuNPs against bacterial strains

Microorganisms	Concentration (μg mL^{-1})
MIC	
E. coli 2443	32
E. coli CS109	32
P. aeruginosa	32
S. enterica	32
K. aerogenes	32
B. subtilis	128
MBEC	
E. coli 2443	256
E. coli CS109	256
P. aeruginosa	128
S. enterica	256
K. aerogenes	256
B. subtilis	512

The Minimal inhibitory concentration of CuNPs

Minimum inhibitory concentration (MIC) of CuNPs was determined using the micro-broth dilution method (CLSI standard) with the serially diluted CuNPs from stock (1 mg/mL). Bacterial cells grown up to an OD_{600}~ 0.2 from the overnight cultures were used as inoculum. The 96-well plates were incubated at 37°C for 18 h before checking the reading microplate reader.

Minimal biofilm eradication concentration (MBEC) of CuNPs

At day one, the biofilm was set up in a static condition for 24 h in LB Broth in 24 wells microtiter plates, followed by the discard of the spent media and wash gently with sterile physiological saline (0.9%) twice, at day two. The fresh media with varying concentrations of nanoparticles were added and incubated for 24 h. At day three, the spent media was discarded, and biofilm was washed with sterile saline. The fresh media was added, and the plate was incubated for 4 to 6 h. After incubation, the growth was analysed to evaluate the MBEC. The staining of the cells was done with 1% TTC (Triphenyl tetrazolium chloride) to determine the growth of the cells and OD_{592} was measured in ELISA multi-plate reader.

Cytotoxicity studies of nanoparticles using MTT assay

Copper nanoparticles were evaluated for their cytotoxicity against macrophage cells (RAW 264.7) by MTT assay. RAW 264.7 cells (2.5×10^5 cells/mL) in DMEM were seeded into polystyrene coated 96-well microtiter plates (Tarsons) and allowed to adhere for 5 h at 37°C in 5% CO_2 incubator. These cells were then incubated with increasing concentrations of copper nanoparticles (10, 20, 30, 60 μg/mL). Wells with only RAW 264.7 in DMEM media was maintained as a control. The plate was then incubated for 24 h under the same conditions. Then, the cells were treated with 20 μL (10 mg/mL) 3-(4,5-dimethylthiazol-2-yl)-2,5-diphenyltetrazolium bromide or MTT (0.4 mg/mL final concentration) in each well and the plate was further incubated for 4 h. Finally, formazan crystals so formed within the cells were dissolved using dimethyl Sulphoxide (DMSO) and the absorbance was measured using a plate reader at OD_{595}.

Mechanism of action of CuNPs against E. coli 2443

The mechanism of action of CuNPs was studied

against Gram-negative *E. coli* 2443. Bacterial cells were grown in LB-broth with and without sub-inhibitory concentrations (16 µg/mL) of CuNPs. Then the tubes were incubated overnight at 37°C. The mechanism of action was analysed in three ways; (a) Localization studies of FtsZ and FtsI proteins using Fluorescence microscopy, (b) study of oxidative stress defence genes using semi-quantitative RT-PCR analysis and (c) DNA degradation assay.

Localization studies of FtsZ and FtsI proteins in presence of CuNPs using Fluorescence microscopy

Plasmids pFtsZ-GFP (EC-568) and pFtsI-GFP (EC-572) containing the cell septation protein fused with green fluorescence protein was transformed into competent *E. coli*2443 by heat shock method and positive clones were screened on LB-agar plate containing ampicillin (Amp; 100 µg/mL). The transformed cells were grown overnight in 5 mL LB broth (LBB) with ampicillin and glucose (0.2%). Cells were harvested by centrifuging at 6000 rpm in a tabletop microcentrifuge and washed with LBB/Amp twice to remove the glucose. The cells were re-suspended in LBB/Amp, and 0.1% of inoculum was used to inoculate two sets of 10 mL LBB/Amp, test and control. A control sample contains IPTG (5 µM) while the test sample contains both CuNPs (sublethal concentration; 16 µg/mL) and IPTG. Cells were grown for one h at 37°C and aliquots (500 µL) were taken every 5 min and fixed with formaldehyde (4%). Cells were visualized under the fluorescence microscope using a green filter. Fluorescent image and phase-contrast image of the same field was observed at 100X magnification using immersion oil and multiple images were taken.

RT-PCR analysis

A known anti-oxidative stress defence gene from *M. smegmatis* mc^2155, *ahpC was* selected for this study. The 16S rRNA was used as an internal positive control. The total RNA was isolated from mc^2155 using the manufacturer's instructions (Nucleopore, New Delhi, India).

cDNA synthesis

After confirmation of no genomic DNA contamination by PCR, first-strand cDNA was synthesized following the manufacturer's instructions (Bio Bharti, Kolkata, India). Briefly, the random hexamers, mRNA (1ng) and dNTP mix were heated to 65°C for 5 min followed by quick chilling on ice. The mixture was added with first-strand buffer, 0.1 M DTT, RNase inhibitor and reverse transcriptase and incubated for one h at 42°C in a water bath. The reaction was terminated by heating the reaction mix at 70°C for 15 min. The cDNA templates were amplified using gene-specific primers in a thermocycler (Hamburg-Eppendorf, Hamburg, Germany). The RT-PCR was carried out using the gene-specific primers.

Primers for 200bp segment of *ahpC*(5′GT GTGTCGGTGGACAACGAG-3′ and 5′-GGTCACC GACACGAACTGGA-3′) and 76 bp control fragment 16S rRNA genes (5′-GTGGACTACCAGGGTA TCTAATCCT-3′ and 5′GGGTCTCTGGGCAGTA ACTG-3′) were synthesized. The amplified products were run in 1% agarose gel and analysed.

DNA Degradation assay

The CuNPs mediated reactive oxygen species (ROS) generation inside the cells were tested by DNA degradation assay. The degradation assay was performed on both the bacterial and the mammalian genomic DNA. The assay was optimized for the effective time of action and concentration of the CuNPs. The optimal time of DNA degradation was observed in a reaction mix containing PBS and 200 µM of CuNPs, and by stopping the reaction with 1 M Tris-HCl at regular intervals of 5, 10, 15, 20, 25 and 30 min. All the reactions were performed at RT. The reaction product was resolved on 1% agarose gel and the DNA degradation was viewed in gel doc equipment (UVP Biosciences, India).

Results and discussion:

CuNPs synthesized to have a very small size range

The CuNPs were synthesized by precipitating copper (Cu) in the presence of Thiosalicylic acid and subsequently reduced by hydrazine hydrate. UV-visible spectral analysis of CuNPs was done to analyse the spectral peak during the nanoparticle formation. The UV-visible peak of CuNPs was scanned from 200-800 nm and the copper peak was around 570 nm indicating a red-shift that implied small-sized CuNPs were formed (Fig. 1A). FTIR analysis of CuNPs showed peaks at 600, 1632 and 3454 cm^{-1} that represents Cu-S bonding, carbonyl-stretching and OH-stretching, respectively (Fig. 1B), which indicated the bonding between Cu and sulphur of Thiosalicylic acid. The X-ray diffraction data showed the peak value of planes (111), (200), (220) &

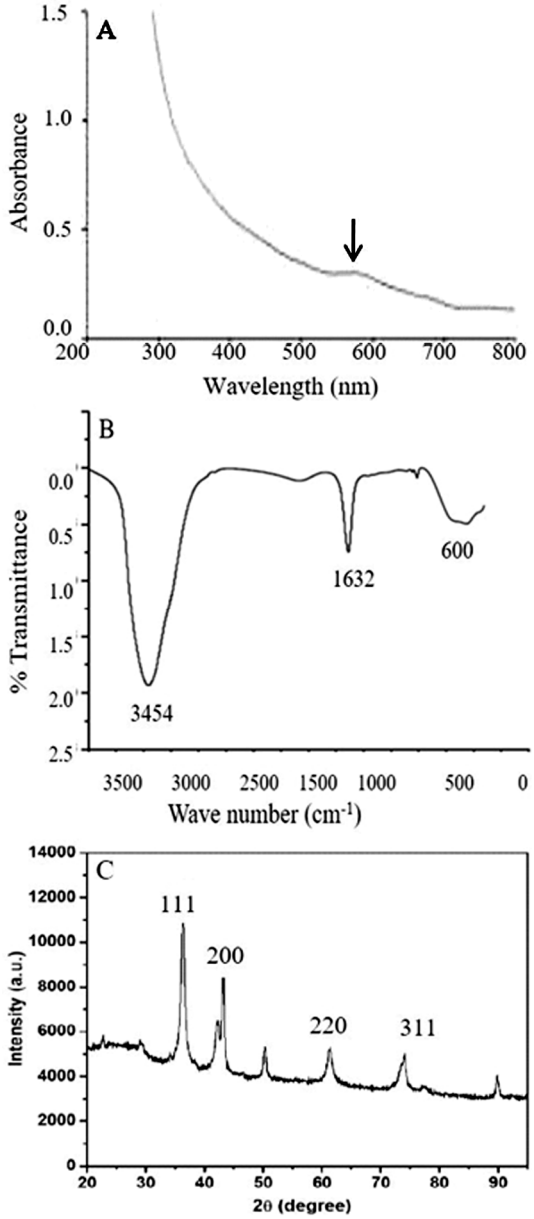

Fig. 1 — Analysis of nano-particle: (A) UV-visible spectrum analysis of CuNPs; (B) FTIR analysis of CuNPs shows there is bonding between Cu and S; and (C) X -ray diffraction pattern of copper nanoparticles

(311) corresponding to the 2θ (theta) values 36.5, 42.4,61.55 and 73.7 that matched to FCC (Face centred cubic) crystals index of CuNPs (Fig. 1C). There were also copper oxide peaks showing the formation of a thin oxide layer that could affect the antimicrobial activity[15].

The CuNPs were also characterized through Dynamic Light Scattering (DLS) analysis that showed the size range between 45-100 nm. However, the HR-TEM analysis revealed the spherical-shaped CuNPs in

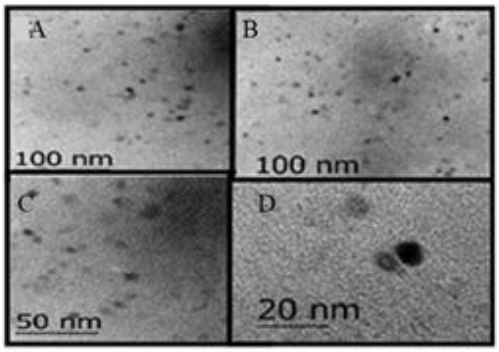

Fig. 2 — HRTEM images of CuNPs shows at different magnifications from 100-20 nm(A-D)

the range from 5-11 nm (Fig. 2A-D) The selected area electron diffraction (SAED) analysis illustrated a prominent crystalline ring pattern (Fig. 3), thus confirming the presence of crystalline CuNPs as shown in histogram (Fig. 4A & B).

CuNPs exerts bactericidal activity on both planktonic and sessile forms of the bacterial population

The minimal inhibitory concentration (MIC) of CuNPs was determined against *E. coli* and other micro-organisms in their planktonic forms. Here, IC_{90} value of the CuNPs was considered where 90% of the visible bacterial growth was inhibited which is shown in MIC values (Table 1). Sensitivity assessment revealed that Gram-negative strains were more susceptible to CuNPs than the Gram-positive ones. This is probably due to the higher penetration of CuNPs through the outer membranes in Gram-negative bacteria. To check whether the CuNPs were effective against the sessile form of bacteria, *i.e.*, bacterial biofilms, minimal biofilm eradication concentrations (MBEC) were determined with CuNPs. The result showed the inhibition in biofilm formation by 90% in 24has revealed by the live-dead staining (Table 1). To check whether the CuNPs were toxic to the host cells, the cytotoxicity of CuNPs was assessed on macrophage RAW 264.7. Though, CuNPs were less toxic at concentrations below 60 µg/mL though the toxicity increased with the higher concentrations (Fig. 4C). The toxicity of the CuNPs to macrophage cells is speculated to be due to the ROS generating property inside the cells[17,18.]

CuNPs degrade genomic DNA of bacterial and mammalian cells by ROS generation*:*

The alkyl hydroperoxide reductase (*AhpC*) is a well-known anti-oxidative stress defence enzyme in

M. smegmatis[19,20]. The gene product of *ahpC* helps to scavenge the ROS species like H_2O_2 and singlet oxygen speciesinside the bacterial cells during oxidative stress. To understand the effect of CuNPs on *ahpC*expression RT-PCR analysis was done[21,22,23,24,25]along with the internal positive control

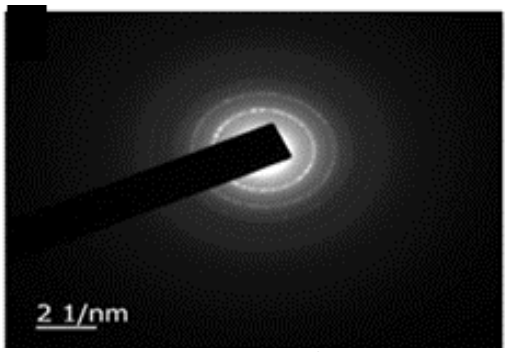

Fig. 3 — SAED pattern of CuNPs

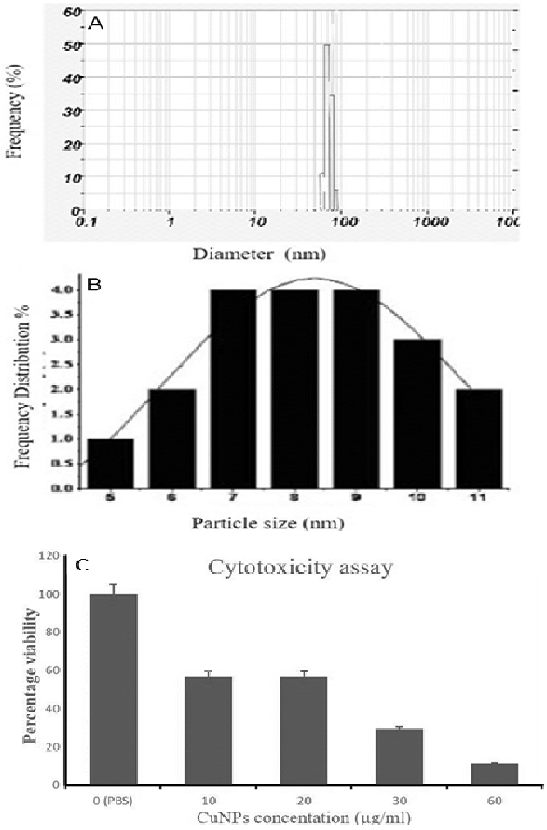

Fig. 4 — (A) Particle size distribution of CuNPs by DLS shows size disribution from 45-100 nm; (B)The histogram of CuNPs; (C) MTT assay of CuNPs against RAW 264.7 cells at various concentrations. The CuNPs were toxic to the RAW cells at higher (60 µg/ML)

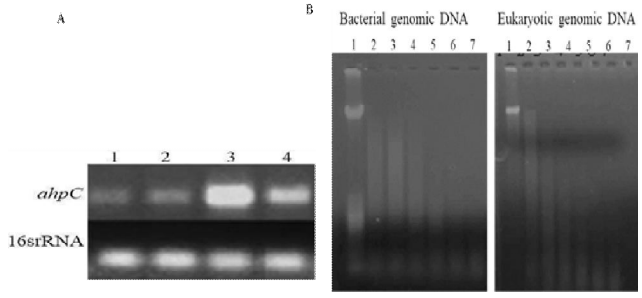

Fig. 5 — (A) RT-PCR analysis of oxidative stress response genes *ahpC*. Lane 1- CuNPs untreated, Lane 2- CuNPs treated overnight, adapted. Lanes 3 & 4, CuNPs and H_2O_2 shock treatment (30 min before harvesting), respectively. Here, 16SrRNA was used as an internal positive control and $H_2O_2$was used as an experimental positive control; (B) Agarose gel electrophoresis (1%) of bacterial and eukaryotic genomic DNA treated with CuNPs. Lane 1 indicates untreated genomic DNA and lanes 2-7 shows genomic DNA treated with CuNPs (200 µM) for 5, 10, 15, 20, 25 and 30 min in presence of bacterial and eukaryotic genomic DNA, respectively

(16S rRNA). We treated the cultures with CuNPs and H_2O_2 (experimental positive control) in two different conditions, adapted (added along with the inoculum) and shocked (added 30 min before harvesting). Interestingly, we observed an increased mRNA level of *ahpC* under the shocked condition when compared to the 16S rRNA and adapted treated condition. The result showed the generation of more ROS in shock treated condition was probably due to less time for the organism to counter the stress. However, adapted treatment had no significant effect (Fig. 5A). The genomic DNA degradation assay of the *M. smegmatis* and mammalian DNA showed higher degradation with 200 µM CuNPs at different exposure time as observed by the increase in degraded DNA (Fig. 5B) Overall, it can be hypothesized that the entry of smaller CuNPs inside the cells can degrade the genomic DNA.

The localization of FtsZ and FtsI proteins were destabilized in the presence of CuNPs:

FtsZ is a tubulin-like protein essentially involved in bacterial cell division, which by localizing as a ring-like structure (Z-ring) at the mid cell pave the septum formation during cell division. Similarly, FtsI is transpeptidase that synthesizes the lateral wall peptidoglycan at the site of formed Z-ring, which eventually generates peptidoglycan layer at the newly formed cell poles [26,27]. If any material inhibits the recruitment of FtsZ, like FtsA and Zip A[28] or its stabilization (ZapA-D)[28,29] or the polymerization

(SlmA, MinC)[30,31,32], the Z-ring would not form and subsequently, FtsI cannot undergo localization at the Z-ring, which in turn stops the cell division. In this situation, the cell would become elongated and finally undergo lysis. To check whether the CuNPs affect the process of cell division, we expressed green fluorescent protein- tagged FtsZ and FtsI from two separate plasmids under the control of *lac* promoter in the *E. coli* 2443cells in presence and absence of CuNPs at a sub-inhibitory concentration (16 µg/mL). The cells without CuNPs treatment showed Z-ring formation at the mid-cell and divide. However, in CuNPs treated cells both FtsZ and FtsI proteins were not precisely localized at the mid-cells and remained scattered in the cytoplasm. After 2 h of incubation, the cells became elongated and the cell density was reduced, possibly indicating some of the cells were lysed as observed through phase-contrast and fluorescent microscopy (Fig. 6A-H). Therefore, we hypothesize that the localization of FtsZ at the mid-cell is inhibited in presence of CuNPs and probably CuNPs act either by binding to FtsZ or binding to some other proteins required for FtsZ localization (see above). Subsequently, in the absence ofZ-ring, it is likely, FtsI might not be localized that eventually inhibits the septum formation which makes the cell elongated that is exactly what we have observed upon CuNPs treatment.

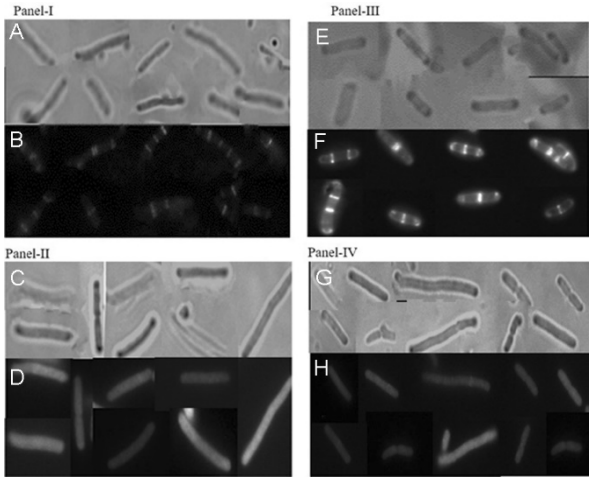

Fig. 6 — Micrographs of the cells showing the effect of a sub-inhibitory concentration of CuNPs (16 µg/mL) on the localization of FtsZ and FtsI in *E. coli* 2443 visualized under 100X magnification. (A & B) Cells expressing FtsZ-GFP; (C & D) FtsZ –GFP expressing Cells treated with CuNPs; (E & F) Cells expressing FtsI-GFP; (G & H) Cells expressing FtsI-GFP treated with CuNPs for Phase-contrast and Fluorescent

Discussion

The CuNPs with a size range between 5-10 nm are synthesized, which are indeed very small in size, and they show excellent antimicrobial and antibiofilm activity against Gram-negative bacteria at a lower concentration. The study on deciphering the mode of the action of CuNPs reveals that the CuNPs interacts with FtsZ and FtsI and prevent septal ring formation[30,31] at the time of cell division in *E. coli* 2443, apart from the other mechanisms like ROS generation and DNA damage. It is also observed in ROS generation assay that there is an elevated expression level of oxidative stress response genes (*ahpC)*[33] which shows elevated ROS production and simultaneous inhibition of cell division which causes cell death. Hence from the results of the present study, it may be concluded that CuNPs can be a potential candidate against Gram-negative strains of bacteria and might be effective against MDR strains.

Conclusion

In a nutshell, we can conclude that CuNPs synthesized in this study have effective antibacterial potential against Gram-negative bacteria. The CuNPs inhibit the cell division process possibly by interfering with FtsZ and kill the bacterial cell possibly by reactive oxygen species (ROS) mediated DNA damage.

Acknowledgment

This work is supported by a research grant from the Department of Biotechnology (DBT), Government of India vide Grant #BT/PR24255/NER/95/716/2017 to ASG. GKNacknowledges IIT Kharagpur for assistantship and Central Research Facility (CRF), IIT Kharagpur.

Conflict of Interest

All authors declare no conflict of interest.

References

1 Levy SB & Marshall B, Antibacterial resistance worldwide: causes, challenges and responses. *NatMed*, 10 (2004) 122.

2 Burda C, Chen X, Narayanan R & El-Sayed M A, Chemistry and properties of nanocrystals of different shapes. *Chem Rev*, 105 (2005) 1025.

3 Da Silva Ferreira V, ConzFerreira ME, Lima LMT, Frasés S, de Souza W & Sant'Anna C, Green production of microalgae-based silver chloride nanoparticles with antimicrobial activity against pathogenic bacteria. *Enzyme Microbe Technol*, 97 (2017) 114.

4 Panáček A, Smekalova M, Vecerova R, Bogdanova K, Roderova M, Kolar M, Kilianova M, Hradilova S, Froning JP, Havrdova M, Prucek R,Zbořil R & Kvítek L, Silver nanoparticles strongly enhance and restore bactericidal activity of inactive antibiotics against multiresistant Enterobacteriaceae. *Colloids Surf B: Biointerfaces*, 142 (2016) 392.

5 Saqib N, Rahim M & Madridge J, Toxicity of Silver Nanoparticles. *Nanotechnol*, 1 (2016) L1.

6 DeekalaV, BabuBK&RudrarajuR, Pharmacological studies of zinc oxide nanoparticles. *Indian J Biochem Biophys*,56 (2019)500.

7 Louis C & Pluchery O, Gold Nanoparticles in the Past: Before the Nanotechnology Era. *Gold nanoparticles for physics, chemistry and biology* (World Scientific,Singapore) 2017, 8.

8 Smail NA, Shameli K, Wong MM, Teow SY, Chew J & Sukri SN, Antibacterial and cytotoxic effect of honey mediated copper nanoparticles synthesized using ultrasonic assistance. *Mater Sci Eng: C*, 104 (2019) 109899.

9 Chen HF, Wu JJ, Wu MY & Jia H, Preparation and antibacterial activities of copper nanoparticles encapsulated by carbon. *New Carbon Mater*, 34 (2019) 382.

10 Sun C, Li Y, Li Z, Su Q, Wang Y & Liu X, Durable and washable antibacterial copper nanoparticles bridged by surface grafting polymer brushes on cotton and polymeric materials. *JNanomater*, 2018 (2018).

11 Kumari SA, Babu BK, Satyanarayana CC, Padma M & Latha BS, Metallopharmaceuticals: Synthesis, characterization and bio-active studies. *Indian J Biochem Biophys*, 56 (2019) 325.

12 Rai M, Ingle AP, Pandit R, Paralikar P, Shende S, Gupta I, Biswas JK & da Silva SS, Copper and copper nanoparticles: role in management of insect-pests and pathogenic microbes. *Nanotechnol Rev*, 7 (2018) 303.

13 Simon AT, Dutta D, Chattopadhyay A & Ghosh SS, Copper Nanocluster-Doped Luminescent Hydroxyapatite Nanoparticles for Antibacterial and Antibiofilm Applications.*ACS Omega*, 4 (2019) 44697.

14 Sreeju N, Rufus A & Philip D, Microwave-assisted rapid synthesis of copper nanoparticles with exceptional stability and their multifaceted applications. *J Mol Liq*, 221 (2016) 1008.

15 Guo Y, Cao F, Lei X, Mang L, Cheng S & Song J, Fluorescent copper nanoparticles: recent advances in synthesis and applications for sensing metal ions. *Nanoscale*, 8 (2016) 4852.

16 Lee Y, Choi J-r, Lee KJ, Stott NE & Kim D, Large-scale synthesis of copper nanoparticles by chemically controlled reduction for applications of inkjet-printed electronics. *Nanotechnol*, 19 (2008) 5604.

17 Shrivastava A, Aggarwal LM, Mishra SP, Khanna HD, Shahi UP &Pradhan S, Free radicals and antioxidants in normal versus cancerous cells—An overview. *Indian J BiochemBiophys*,56 (2019)7.

18 Mistry KN, Dabhi BK&Joshi BB, Evaluation of oxidative stress biomarkers and inflammation in pathogenesis of diabetes and diabetic nephropathy.*Indian J Biochem Biophys*,57 (2020) 45.

19 Bhutia RD, Khandelwal B, Sherpa ML&Singh TA, Oxidation products of DNA, lipid and protein among the individuals progressing towards metabolic syndrome. *Indian J BiochemBiophys*,56(2019) 155.

20 Hutchison JE, The road to sustainable nanotechnology: Challenges, progress and opportunities. *ACS Sustain Chem Eng*, 4 (2016) 5907.

21 Slavin YN, Asnis J, Häfeli UO & Bach H, Metal nanoparticles: understanding the mechanisms behind antibacterial activity. *J Nanobiotechnol*, 15 (2017) 65.

22 Arora V, Ghosh MK, Singh P& Gangopadhyay G, Light regulation of nitrate reductase gene expression and enzyme activity in the leaves of mulberry.*Indian J Biochem Biophys*, 55 (2018) 62.

23 Prajapat P, Singh D, Tripathi S, Patel K, Abbas H& Patel A, Effect of water stress on antioxidative enzymes and glycine betaine content in drought tolerant and drought susceptible cotton (*Gossypium hirsutum* L.) genotypes.*Indian J Biochem Biophys*,55 (2018) 198.

24 Setyawati MI, Fang W, Chia SL & Leong DT, Nanotoxicology of common metal oxide-based nanomaterials: their ROS-y and non-ROS-y consequences. *Asia-Pac J Chem Eng*, 8 (2013) 8205.

25 Mongkolsuk S, Loprasert S, Whangsuk W, Fuangthong M & Atichartpongkun S, Characterization of transcription organization and analysis of unique expression patterns of an alkyl hydroperoxide reductase C gene (ahpC) and the peroxide regulator operon ahpF-oxyR-orfX from Xanthomonas campestris pv. phaseoli. *J Bacteriol*, 179 (1997) 3950.

26 Anderson DE, Gueiros-Filho FJ & Erickson HP, Assembly dynamics of FtsZ rings in Bacillus subtilis and *Escherichia coli* and effects of FtsZ-regulating proteins. *J Bacteriol*, 186 (2004) 5775.

27 Bi E & Lutkenhaus J, FtsZ ring structure associated with division in *Escherichia coli*. *Nature*, 354 (1991) 161.

28 Pichoff S & Lutkenhaus J, Unique and overlapping roles for ZipA and FtsA in septal ring assembly in *Escherichia coli*. *EMBO J*, 21 (2002) 685.

29 Durand-Heredia JM, Helen HY, De Carlo S, Lesser CF & Janakiraman A, Identification and characterization of ZapC, a stabilizer of the FtsZ ring in *Escherichia coli*. *J Bacteriol*, 193(2011) 1405.

30 Durand-Heredia J, Rivkin E, Fan G, Morales J & Janakiraman A, Identification of ZapD as a cell division factor that promotes the assembly of FtsZ in *Escherichia coli*. *J Bacteriol*, 194 (2012) 3189.

31 Bernhardt TG & De Boer PA, SlmA, A nucleoid-associated, FtsZ binding protein required for blocking septal ring assembly over chromosomes in *E. coli*. *Mol cell*, 18(2005) 555.

32 Lutkenhaus J, Assembly dynamics of the bacterial MinCDE system and spatial regulation of the Z ring. *Annu Rev Biochem*, 76 (2007) 539.

33 Wang L, Hu C & Shao L, The antimicrobial activity of nanoparticles: present situation and prospects for the future. *Int J nanomed*, 12 (2017) 1227.